In situ mass spectrometry in a 10 Torr W chemical vapor deposition process for film thickness metrology and real-time advanced process control

Soon Cho, Laurent Henn-Lecordier, Yijun Liu, and Gary W. Rubloff[a)]
Department of Materials Science and Engineering and Institute for Systems Research, University of Maryland, College Park, Maryland 20742

(Received 3 October 2003; accepted 9 February 2004; published 13 April 2004)

In situ mass spectrometric sensing has been implemented in a 10 Torr H_2/WF_6 W chemical vapor deposition process as a real-time process and wafer state metrology tool. Dynamic sensing through the process cycle reveals HF byproduct generation as well as H_2 and WF_6 reactant depletion as real-time quantitative indicators of deposition on the wafer. Thickness metrology is achieved by integrating the HF byproduct signal through the process cycle and comparing it to post-process measurements of film weight. To evaluate the quantitative precision of this metrology, multiwafer runs have been performed under different sets of conditions: (1) fixed process conditions, (2) intentionally introduced run-to-run process temperature drift, and (3) run-to-run deposition time variation. These results demonstrate that real-time thickness metrology is achievable at a level of 1% or better in two application settings: (1) when an essentially fixed process recipe is employed, as in high-volume manufacturing; and (2) when more substantial changes in process recipe are explored, as in a development environment. *In situ* mass spectrometry presents an attractive option for real-time advanced process control with the prognosis for real-time course correction demonstrated here and its already established benefit to fault detection and classification. © *2004 American Vacuum Society.* [DOI: 10.1116/1.1695332]

I. INTRODUCTION

Advanced process control (APC) has become a critical enabling technology for the semiconductor manufacturing industry, enhancing productivity and profitability. The two primary thrusts of APC, namely course correction and fault management, have different goals and attributes.[1–7] Course correction is intended to adjust process parameters so that product quality is maintained in spite of short-term variability and long-term drift in process and equipment behavior, while fault management is aimed at identifying equipment problems that would cause such variability and repairing them in an optimal time frame.

Real-time fault detection, based on *in situ* sensors, has already become a widely accepted practice in semiconductor manufacturing to monitor real-time performance of tools in order to minimize the number of misprocessed wafers. By immediate identification and response to known process and equipment faults, this first component of fault management provides substantial value to manufacturing productivity, and it has been widely implemented using *in situ* sensors, particularly using mass spectrometry [or residual gas analysis (RGA)]. Other aspects of fault management are more challenging and will thus require more sophisticated approaches, including more general fault classification (where sensor signals do not readily distinguish the cause of faults), and fault prognosis for optimal scheduling of tool maintenance actions.

Course correction has been widely adopted for manufacturing in the form of run-to-run (R2R) control (or wafer-to-wafer control). Guided mainly by in-line metrology (e.g., x-ray reflectance, x-ray fluorescence, four-point probe, etc.)[8] rather than by *in situ* sensors, R2R control can rely on well-developed metrology tools that are not typically integrated into the process equipment, and it provides a powerful strategy to compensate for long-term systematic process drift using both feedback and feedforward control. In contrast, APC course correction based on *in situ* sensors is only beginning to emerge as a significant component of overall APC strategy in the industry,[9] because it requires *in situ* metrology with sufficient precision to enable subtle quantitative process adjustments. On the other hand, if adequate *in situ* metrology were available, it would present a major benefit not only as an alternative to in-line metrology for R2R course correction, but particularly for real-time course correction. *In situ* metrology could then be employed to compensate for random short-term variability that occurs within a process step, as well as for long-term systematic process drift, and it would complete a more powerful APC strategy that includes tool-level real-time control (course correction and fault detection) in a larger context of hierarchical APC.[1]

In principle, *in situ* sensors can provide the metrology needed for either R2R or real-time course correction. *In situ* sensors have been utilized in R2R control (e.g., in CMP and lithography processes[3]) and in selected applications for real-time control (e.g., for interferometric etch end-point control and rapid thermal processing). However, *in situ* sensors have seen only limited application for material deposition processes, particularly for mainstream Si technology applications such as chemical vapor deposition (CVD), despite the potential benefits.[1–6] While several *in situ* real-time sensing

[a)]Electronic mail: rubloff@isr.umd.edu

techniques have been investigated for process monitoring, including quadrupole mass spectrometry,[10–18] acoustic sensing,[19–22] UV spectroscopy,[22,23] and Fourier transform infrared spectroscopy,[24,25] a primary limitation in employing such techniques for real-time manufacturing course correction has been the lack of demonstrated metrology precision sufficient to deliver real value in manufacturing.

Our research group has been developing such real-time *in situ* sensing methodologies for CVD process diagnostics, metrology, and APC course correction, using quadrupole mass spectrometry and other chemical sensors.[10–16,19] In recent years, our investigations have focused on W CVD processes with the primary goal of improving the metrology to a sufficient precision—taken as about 1%—that it would be viable for CVD thickness control in high-volume manufacturing, as either R2R or real-time control.[10–13,19] This target is consistent with metrology requirements in the 2002 ITRS roadmap: 4% 3σ for gate dielectric and 10% 3σ for barrier layer at 4–7 nm.[7] We report here advances in the precision of real-time, *in situ* CVD thickness metrology that clearly exceed the 1% target we have been seeking.

II. BACKGROUND

In recent years, we have reported promising results in low-pressure W CVD using both H_2/WF_6 (hydrogen reduction)[11–13,19] and SiH_4/WF_6 (silane reduction)[10] processes. In the case of H_2 reduction at 0.5 Torr, in agreement with the widely accepted reaction mechanism[26]

$$3H_2 + WF_6 \rightleftarrows 6HF_{(g)} + W_{(s)}, \quad (1)$$

we observed H_2 reactant depletion and volatile HF byproduct generation using *in situ* downstream mass spectrometry. Time integration of these mass spectrometry signals, together with post-process *ex situ* film weight measurement, provided a working metrology model such that real-time mass spectrometry signals could be used to predict in real time the average W film thickness deposited on wafer. In this case, the metrology result based on HF byproduct generation signal yielded an average uncertainty on the order of 7%.[11] This was similar to other results obtained by acoustic sensor measurements carried out for the same processes.[19] The precision of both mass spectrometry- and acoustic sensor-based metrologies was limited primarily by the low conversion (or utilization) rate of the reactants (~3%) achieved for this process chemistry, temperature regime, and low-pressure (sub-Torr) operation of the reactor. Our analysis concluded that the metrology was limited by the conversion rate of reactants (since it was based on byproduct generation or reactant depletion) and that higher reactant conversion rates (~30%, as commonly experienced in manufacturing applications such as blanket W CVD at ⩾50–100 Torr) would significantly improve the sensor signal-to-noise ratio and thus the metrology accuracy. An additional drawback resulting from the low conversion rate of the sub-Torr process was that an additional mass spectrometry measurement was necessary (with the wafer at room temperature and process gases flowing) in order to calibrate and compensate for a background signal associated with reactant adsorption and reaction on chamber walls;[11] needless to say, any such background calibration step would be absolutely unacceptable in manufacturing.

In order to improve the metrology precision and demonstrate its suitability for APC, we then investigated the silane reduction process,[27] knowing that SiH_4 is a more efficient reducing agent, as follows:

$$3SiH_4 + 2WF_6 \rightleftarrows 6H_{2(g)} + 2W_{(s)} + 3SiF_{4(g)}. \quad (2)$$

This led to a reasonable conversion rate (~20%) and a thickness metrology precision of order 1%–2%, and we demonstrated real-time end-point control of film thickness to within 3% of target in the face of 10% open-loop wafer-to-wafer thickness variation.[10]

We have modified our W CVD reactor to enable higher pressures (to ~100 Torr total pressure) in the range typically employed in W CVD manufacturing processes and reconfigured our mass spectrometry sampling system accordingly, as described in Sec. III. In this article, we present metrology results for the H_2/WF_6 chemistry (hydrogen reduction) at a higher pressure of 10 Torr, under three sets of conditions: (1) a fixed process condition, (2) intentionally introduced R2R process temperature drift, and (3) intentionally introduced R2R deposition time variation. The results demonstrated quantitative thickness metrology with precision of 1% or better. Following a description and analysis of these results, we discuss the prognosis for applying this methodology in real manufacturing environments.

III. EXPERIMENTS

A. 10 Torr blanket W CVD: Equipment and process

Experiments were carried out within a single-wafer CVD reactor on a manufacturing scale cluster tool (Ulvac model ERA1000). Originally, there were two single-wafer reactors on the tool, both of which were configured for sub-Torr pressure selective W CVD process.[11,28] In order to enable high-pressure processing (i.e., 10 Torr or above), modifications of the existing tool configuration were necessary. First, a low-conductance throttle valve (0.07–24 L/s) and associated exhaust plumbing was installed for pressure control at or above 10 Torr, in parallel with the existing system (1.5–900 L/s) for use at low pressure. Second, the wafer heating mechanism was converted from the existing lamp heating to a resistive substrate heating design, which reduced heating of the quartz showerhead and associated deposition on it.

The reactor employs water-cooling of the walls to avoid excessive precursor condensation and reaction. Separate inlets are provided for the H_2 and WF_6 gases to minimize gas phase reaction, with the H_2 introduced through a circular quartz showerhead located 5 in. above the wafer, and the WF_6 introduced through a side slot located at wafer height, as seen in Fig. 1. The pumping package for the reactor includes a roots blower pump backed up by a mechanical rotary pump for process pumping, and a turbomolecular pump for maintaining high vacuum cleanliness in system idle mode. The process pressure is controlled by the downstream

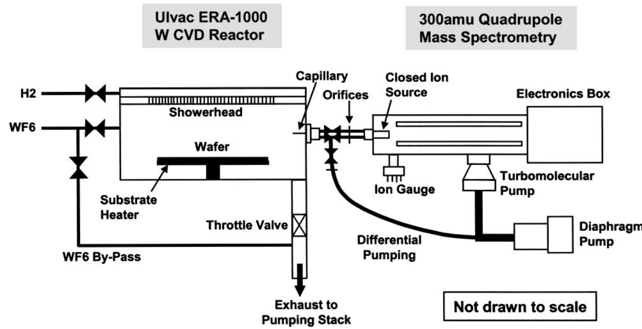

FIG. 1. Schematic of the 300 amu *in situ* quadrupole mass spectrometry gas sampling system (Inficon model CIS2™) attached to the Ulvac ERA1000 cluster tool reactor for H_2/WF_6 W CVD process at 10 Torr. Not drawn to scale.

low-conductance throttle valve (described earlier) driven by a capacitance diaphragm gauge. Individual gas flows are regulated by mass flow controllers.[11,28,29]

Blanket W CVD processes were carried out at 10 Torr using H_2/WF_6 gases with 6:1 flow ratio. Deposition temperature and time were intentionally varied to investigate the metrology capability under different process conditions, including nominally stable situations and wafer sequences in which conditions were intentionally varied to simulate process drift. Experiments covered the range of deposition temperatures of 340–400 °C and times of 5–15 min. Temperatures are reported here as set-point values for the substrate heater control system, in which substrate heater temperature was measured by a thermocouple. The temperature on the wafer, as measured by an instrumented wafer with thermocouple sensors, was 10–20 °C lower than these set-point values. Deposition times as reported include the time required to achieve nominal process pressure as well as the raw process time at 10 Torr. Most experiments consisted of single-wafer processing of ten-wafer batches.

Experiments began with 1–2 h of reactor wall conditioning (dependent on prior experiments) achieved by flowing the WF_6 and H_2 gases at 10 Torr and room temperature. This conditioning period was effective in reducing the H_2O contamination level and passivating the chamber walls in the reactor system.[11] In order to monitor the progress of reactor conditioning, H_2O partial pressure as well as WF_6/WOF_4 ratio were monitored using the same mass spectrometry used for process sensing. Following the conditioning period, the reactor was purged with N_2 while the substrate heater temperature was ramped to the desired process temperature; this typically lasted over 30 min, depending on the process temperature set point.

Si wafers 4 in. in diameter were used in our experiments. Prior to each run, the wafer was prepared by immersing it in 10% buffered HF solution for 20 min to remove the native oxide, rinsing with deionized water (resistivity 18.4 MΩ cm), and blow drying with N_2. It was then transferred into the CVD reactor via a high-vacuum load-lock chamber and an automated wafer-handling robot. After a 2 min delay to enable stabilization of wafer temperature, the deposition process was initiated. The process recipe included three steps:

(1) *Reactor filing period*, during which 900 sccm of H_2 and 150 sccm of WF_6 were introduced into the reactor for 18 s. The high flow rates (compared to those during the following raw process time at 10 Torr) were necessary to ramp the pressure in the 25 L reactor up to 10 Torr in a reasonably short period of time.
(2) *Raw process time at 10 Torr*, during which H_2 and WF_6 gas flow rates were now reduced to 60 and 10 sccm, respectively. The low flow rates (compared to those during the previous reactor filling period) were used to increase the residence time of the process gases and thus their conversion (or utilization) rate. The higher conversion rate enhances the RGA metrology signals associated with reactant depletion and byproduct generation, as discussed in Sec. II. The raw process time studied in this article varied between 5 and 15 min.
(3) *Reactor pump-down/purge period*, during which the reactor was pumped down and then purged with N_2 at 100 Torr for 85 s and at 10 Torr for 60 s. Although these purge steps were not required by the deposition process itself, they were useful for detecting any long-term or R2R sensitivity drift in the sensor. The processed wafer was then unloaded, and a new one was introduced into the reactor following the same sequence of steps just described.

Following each wafer run, the amount of W deposited on the wafer was determined by an *ex situ* wafer weight measurement using a microbalance (0.0001 g resolution). The average film thickness was then deduced based on the known W bulk density of 19.35 g/cm^3. Our film weight measurement data carried approximately ±0.1% (or 0.0005 g) error for the entire range of film thickness reported here due to uncertainty in the measurement technique.

B. Real-time, *in situ* process sensing by mass spectrometry

The mass spectrometry sampling system is shown schematically in Fig. 1. Residual process gases were sampled directly from the downstream side of the reactor via a 0.020-in.-inner-diameter (i.d.)×10-cm-long stainless steel capillary, which resulted in a pressure drop from the process pressure of 10 Torr down to 1 Torr behind the capillary. Most of this gas was then pumped away by a bypass differential pumping to the foreline of the diaphragm pump (the backing pump for the mass spectrometer turbo pump), leaving a small fraction of the gas to be directly sampled through a 20-μm-i.d. orifice into the closed ion source region of the mass spectrometer (Inficon model CIS2™, 300 amu quadrupole mass spectrometer).

The appropriate size capillary–orifice combination for conductance control effectively reduced the sampled gas pressure from the viscous flow regime (10 Torr) to the molecular flow regime (1 Torr). The bypass differential pumping technique enabled us to actively withdraw gases from the process through the sampling system. Both of these sampling

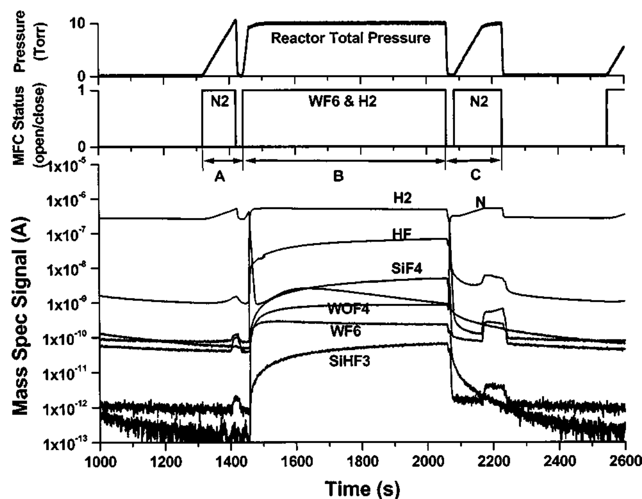

FIG. 2. *In situ* RGA signals from mass spectrometry, indicative of the gas composition inside the reactor, were acquired together with the equipment state signals from the tool control in real time. Step A indicates the pre-process N_2 purge period. Step B indicates the deposition cycle which includes the reactor filling period and the raw process time at 10 Torr. Step C indicates the reactor pump-down and the final N_2 purge period. The substrate heater temperature was nominally maintained at 390 °C at all times for this particular run through steps A, B, and C.

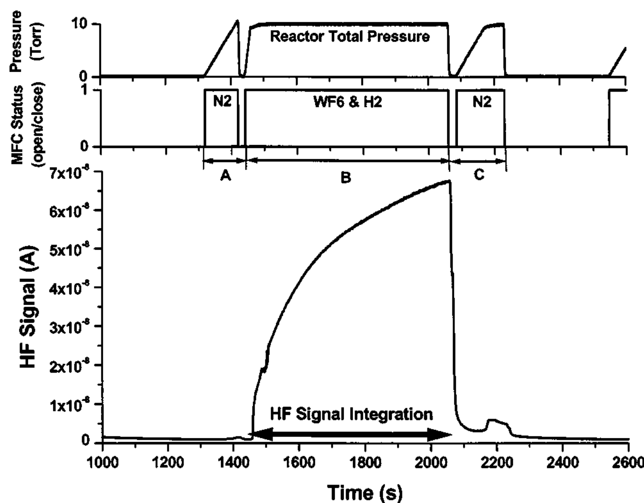

FIG. 3. *In situ* HF byproduct generation signal obtained in real time during the deposition cycle. Metrology signal was obtained by integrating the HF signal over the entire deposition period (step B), which included the reactor filling period as well as the raw process time at 10 Torr. This particular example is taken from the same run as in Fig. 2.

techniques, as well as the location of the sampling capillary (i.e., downstream but close to the wafer), were critical in achieving fast response time in process sensing. In addition, to minimize the effect of adsorption and reactions of WF_6 and HF on the stainless steel surfaces at room temperature, wall areas of the sampling system were kept heated at 65 °C.

The filament current in the closed ion source was kept at 200 μA, while the electron energy was maintained at 40 eV, which provided adequate sensitivity and minimum parasitic reactions within the closed ion source region. Electron multiplier detection was used at an acceleration voltage of 1600 V to enhance the signal-to-noise ratio.

IV. RESULTS

A. Metrology development

In situ mass spectrometry sensing of the 10 Torr W CVD process as described in Sec. III has provided us with dynamic, real-time gas phase chemical signals as a function of the process cycle. Figure 2 shows characteristic ion current signals from the H_2 and WF_6 reactants, HF byproduct, N_2 purge gas, as well as other species used to monitor reactor cleanliness (H_2O,WOF_4) and parasitic reactions on the quartz showerhead (SiF_4,$SiHF_3$). Partial pressures of these species exhibit strong time dependence through the process cycle, including background levels before and after the single-wafer process, N_2 purge cycles before (step "A") and after (step "C") the process, and dynamics within the process itself (step "B"). In particular, during the process ("B"), the reactant gases (H_2 and WF_6) and the reaction byproduct species exhibit different dynamics. This is primarily a consequence of the reactor residence time, which determines the rate at which reaction byproduct generation and reactant depletion attain steady state.

Among the various chemical signals, the characteristic RGA signals indicating H_2 and WF_6 reactant depletion and HF byproduct generation were considered good candidates for thickness metrology based on the known reaction mechanism and stoichiometry described by Eq. (1). We found that the HF byproduct generation signal at 20 amu, integrated through the entire deposition cycle, provided us with the best metrology accuracy. Figure 3 shows the HF byproduct signal, which we integrated through the process cycle to obtain a thickness metrology.

B. Run-to-run process drift and metrology under fixed process conditions

A batch of ten wafers was processed under identical nominal process conditions at 10 Torr, 400 °C, for a fixed deposition time of 640 s. Despite the fixed process condition specified by the tool set points, an average of 1.18% R2R process drift was manifested in the post-process film weight measurement, as seen in Fig. 4. The actual variation in film weight was 3.0 mg on average, which corresponds to 199 Å in terms of film thickness as estimated assuming the bulk density of W to be 19.35 g/cm^3. Such R2R process drifts can have significant impact on manufacturing yield and have been a strong motivation for industry adoption of R2R control as a prime component of APC. The drift appears to include random as well as systematic components, with the deposited film weight exhibiting a systematic drift of 0.40% for each successive wafer. We attribute this R2R drift to increased W nucleation on the quartz showerhead and chamber walls for each successive run leading to easier W deposition at those nonwafer surfaces, as discussed further in the next set of experiments.

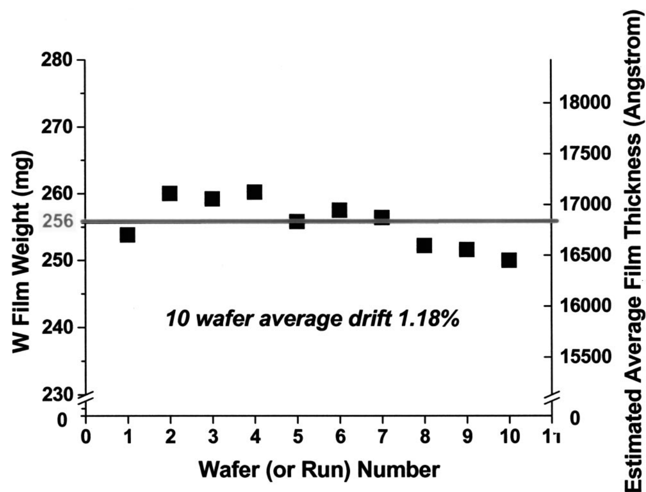

FIG. 4. A batch of ten wafers processed (one wafer per run) under identical nominal process condition at 10 Torr, 400 °C for a fixed deposition time of 640 s. R2R systematic drift as well as random variations in the processes were manifested by the post-process W film weight measurement with an average R2R variation of 1.18%.

Despite the unintentional R2R drift present in the process, real-time, *in situ* metrology based on time-integration of the HF byproduct signal reveals the drift directly and is quantitatively correlated with the post-process film thickness measurements, as seen in Fig. 5. A linear regression fit was made through the ten-wafer run, and the average difference between the actual film weight measurement and the predicted value from the regression model provided us with a metric for quantitatively determining our metrology accuracy. We called this metric the *average uncertainty*, which for this batch of ten wafers was found to be 0.56% over the total range of film weight variation of 10.2 mg (or 671 Å in terms of estimated film thickness).

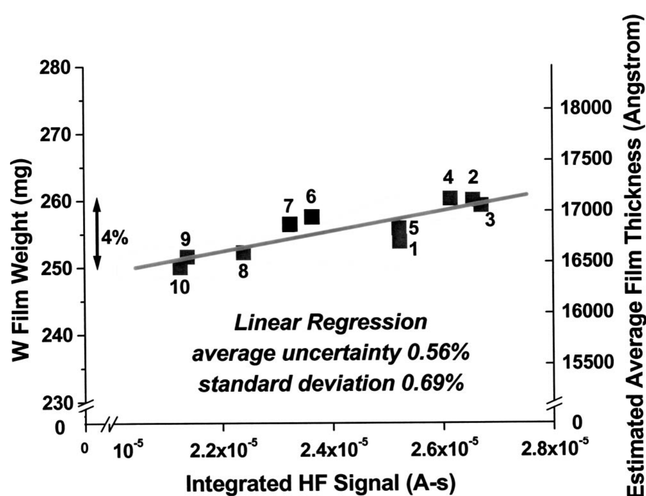

FIG. 5. Film thickness metrology model based on *in situ* time-integrated HF signal and *ex situ* W film weight measurement for the ten wafers processed under nominally fixed process condition as shown in Fig. 4. First-order linear regression fit yielded an average uncertainty of 0.56% within the corresponding range of film weight variation of 10.2 mg (or 671 Å in terms of estimated film thickness).

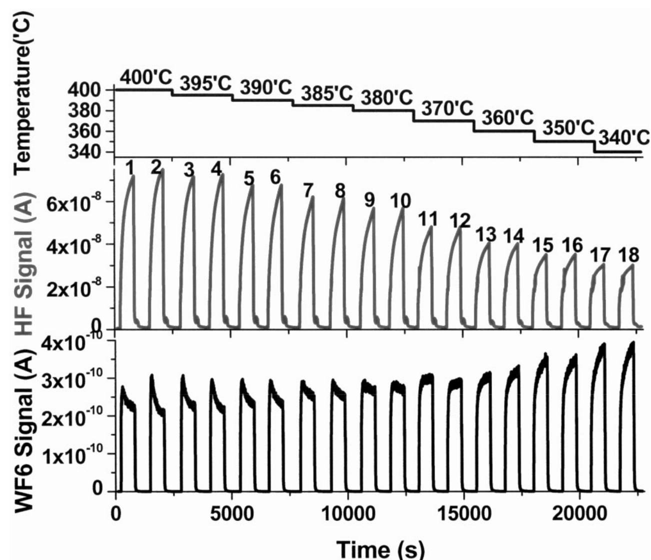

FIG. 6. A batch of 18 wafers processed (one wafer per run) with an intentionally introduced R2R drift in wafer temperature for every two wafers. R2R changes in magnitude as well as shape of the HF byproduct generation and the WF_6 reactant depletion signals were observed. Wafer (or run) numbers are indicated above each corresponding HF signal.

C. Intentionally introduced run-to-run temperature drift and metrology

In order to understand the effects of equipment and process drift and to develop a precision real-time, *in situ* metrology, a temperature drift was intentionally introduced during processing of an 18-wafer batch, maintaining a fixed deposition time of 618 s. We chose to introduce the drift in the form of variation in wafer temperature because it is one of the key equipment parameters that are often susceptible to drift, directly affecting the deposition process and consequently the film thickness. Here, the temperature set point was first reduced for every two wafers by 5 °C from 400 to 380 °C, then by 10 °C from 380 to 340 °C. Figure 6 shows the variation in HF byproduct generation and WF_6 reactant depletion signals with the temperature drift.

The effects of temperature drift on the process are clearly seen in the mass spectrometry signals. With lower process temperature, the magnitude of the HF byproduct signal decreased, while maintaining an approximately constant line shape. Because the HF signal is entirely associated with the reaction byproduct and the reactor residence time was constant, we expect the HF signal shape to be maintained as its magnitude changes. In contrast, the line shape for the WF_6 reactant changes appreciably with lower wafer temperature. At high temperatures (e.g., 400 °C) the WF_6 line shape initially reflects introduction of the gas, but is quickly followed by intensity reduction associated with reactant (WF_6) depletion. The shape of WF_6 depletion mirrors the growth of HF byproduct concentration on a time scale associated with the reactor residence time. As seen for later wafers in the experiment, lower temperatures (e.g., 340 °C) cause a noticeable decrease in the magnitude of the depletion, since the reaction rate is lower. As the depletion rate decreases, the line shape

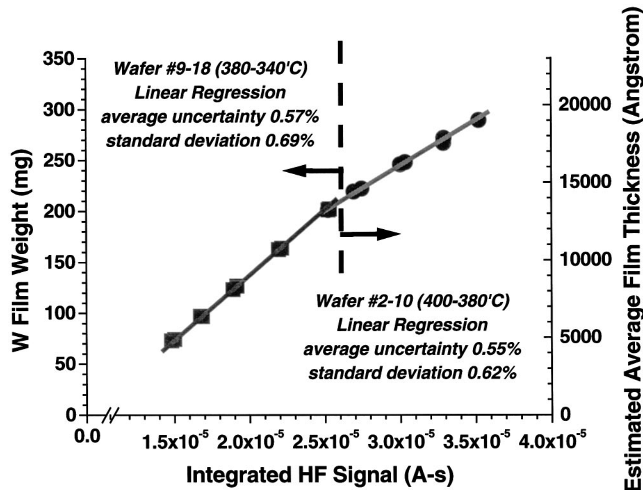

FIG. 7. Film thickness metrology model based on *in situ* time-integrated HF signal and *ex situ* W film weight measurement for the 18 wafers processed under R2R temperature drift as shown in Fig. 6. Note that the first wafer of the batch was excluded for metrology purposes due to the first-wafer effect, as discussed in other publications (see Ref. 10). For metrology purposes, two separate local regions were distinguishable at different temperature ranges, both of which displayed an average uncertainty on the order of 0.5% from linear regression fit as indicated. The corresponding range of film weight variation (or estimated film thickness) was 87.9 mg (or 5783 Å) for wafers #2–#10 and 129.3 mg (or 8508 Å) for wafers #9–#18.

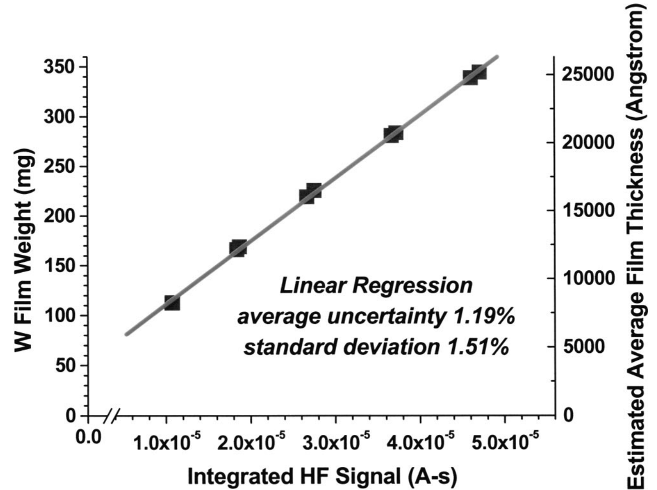

FIG. 8. Film thickness metrology model based on *in situ* time-integrated HF signal and *ex situ* W film weight measurement for ten wafers processed at 390 °C and 10 Torr for five different deposition times (two wafers/runs for each deposition time). First-order linear regression fit yielded an average uncertainty of 1.19% within the corresponding range of film weight variation of 231.9 mg (or 15 260 Å in terms of estimated film thickness).

of the WF_6 reactant partial pressure becomes similar to that expected for gas introduction to the reactor in the absence of chemical reaction.

The post-process *ex situ* measurement of W film weight and the estimated film thickness have been plotted against the integrated HF byproduct signal in Fig. 7. Clearly, there is a strong correlation between the *in situ* thickness metrology signal and the post-process film thickness measurement, and correspondingly the *in situ* measurement provides an accurate prediction of the film thickness even over a large dynamic range of thickness (~4×, or 14 230 Å) and significant temperature range (60 °C). Because the data suggest two regimes of metrology behavior corresponding to two different temperature ranges (wafers #2–#10 over 400–380 °C and wafers #9–#18 over 380–340 °C), we carried out linear regression fits to each region, resulting in an average uncertainty on the order of 0.5% for each region. Note that the range of variation in film weight and thickness is large for each range: 87.9 mg or 5783 Å for wafers #2–#10, and 129.3 mg or 8508 Å for wafers #9–#18. We have obtained similar metrology accuracy using *in situ* acoustic sensing for the same set of experiments.[29]

The metrology demonstrated in Figs. 6–7 is significant for both manufacturing and for process development. For manufacturing one seeks a real-time, *in situ* metrology to compensate for small variations in process due to systematic equipment drift, so the metrological precision of about 0.5% is promising for APC course correction, either R2R control[12,13] or real-time end-point control.[10] Typical targets for APC course correction in manufacturing would be variations of order a few percent, for which the local metrology in Fig. 7 would be very suitable. In contrast, larger variations might well be identified as faults requiring response in terms of equipment repair.

For process development, one would like a metrology which can accommodate experimentation over a wider range of possible process parameters. Within each of the two broad regimes indicated in Fig. 7, the mass spectrometry-based metrology delivers high precision, and a model consisting of both linear regressions linked at the dashed line in Fig. 7 carries comparable precision; thus, the metrology can assist process optimization activities in development as well. We believe the nonlinearity seen in Fig. 7 over a very broad dynamic range of film thickness (and significant process temperature variation) is likely a consequence of W deposition on nonwafer surfaces, which is not accounted for by the post-process film weight measurement. For example, at higher temperatures W nucleation and deposition on the showerhead and chamber walls become more significant, resulting in an increase in the mass spectrometry signal which is not reflected in the post-process film weight measurement.

D. Intentionally introduced run-to-run process time drift and metrology

In order to explore the use of deposition time as our control variable for real-time film thickness control, experiments were carried out by introducing an intentional R2R variation in process time under otherwise fixed conditions. Ten wafers were processed at 390 °C and 10 Torr for five different deposition times in the following order 618, 468, 768, 318, and 918 s, allocating two wafers for each deposition time. HF byproduct generation signal has been integrated over the respective duration of deposition cycle and correlated to W film weight measurement data as shown in Fig. 8. A first-order linear regression fit through the data yielded an average uncertainty of 1.19%, and a second-order polynomial expres-

sion yielded a better fit of 0.48% average uncertainty. The range of deposition times was varied by 3×, leading to a comparable dynamic range of film thicknesses, associated with a 231.9 mg variation in film weight and a film thickness variation of 15 260 Å.

Here again, we explored a much larger variation in process metrics (thickness) than would be a target for APC course correction in manufacturing, so that the benefits of a higher-order fitting model are not surprising. In any case, real-time, *in situ* thickness metrology derived from mass spectrometry data is again capable of precision better than 1%, indicating value for APC course correction in either R2R or real-time end-point control.

V. DISCUSSION

A. Effect of reactant conversion rate on mass-spectrometry-based thickness metrology

We have, here and previously, investigated the use of mass spectrometry as a real-time, *in situ* sensor for CVD thickness metrology based on the sensor's ability to monitor byproduct generation and reactant depletion. In our previous studies using low-pressure W CVD processes with different reaction chemistries (i.e., H_2 reduction and SiH_4 reduction of WF_6), reactant conversion rates were low: ~3% for H_2 reduction process[11] and ~20% for SiH_4 reduction process.[10] In turn, this limited the metrology accuracy to ~7% and ~2%, respectively, which in turn limited the efficacy of both R2R[12,13] and real-time control.[10]

With the significantly higher reactant conversion efficiency (~30%) obtained in this work by using a higher pressure process, we were able to improve the metrology precision to better than a 1% level (and more typically 0.5%). This improvement is attributed to the nearly 10× increase in byproduct generation and reactant depletion rates for the process as compared to previous low-pressure processes. Conversion rates in the range 30%–40% are common in many CVD manufacturing processes, and of course high conversion rates are desirable in terms of the economic and environmental costs of excessive reactant consumption. Accordingly, we expect that the high precision of mass spectrometry-based thickness metrology demonstrated here can be duplicated in manufacturing, thereby enabling new domains of APC course correction for R2R and real-time control.

B. Prognosis for application in manufacturing

Advances in APC depend on availability of suitable metrology tools and implementation of control strategies to exploit the metrology.[4–7] The results presented here and in our previous work have shown that *in situ* mass spectrometry sensing can be used in CVD processes to provide real-time quantitative thickness metrology from measurement of reactant depletion and byproduct generation.[10–16] We have demonstrated that the sensor system can provide metrology signals with high precision, better than 1% average uncertainty, and that predictive models can be generated such that these sensor signals deliver corresponding predictive precision as needed to drive control actions, including R2R control[12,13] and real-time end-point control.[10] This achievement for real-time, *in situ* chemical sensors promises real benefit for application in manufacturing from several perspectives.

First, the precision of this thickness metrology, 0.5%–1.0% average deviation (1σ), is consistent with the requirements of the 2002 International Technology Roadmap for Semiconductors, which specifies 3σ thickness control of 4% and 10% for gate dielectric and interconnect diffusion barriers, respectively.[7]

Second, we believe that the techniques pursued here will perform better (i.e., with higher metrological precision) when implemented in manufacturing. Our progress in improving precision from mass spectrometry sensing has resulted primarily from two factors, processes with acceptably high reactant conversion rates and equipment conditioning. The former has been discussed in Sec. V A. Because reactive chemical processes, particularly with CVD sources, are often accompanied by adsorption and reaction processes on internal system walls, it was necessary to implement conditioning cycles of gas flow to stabilize these reactions. In manufacturing tools at wafer throughputs far larger than achievable in our experiments (ten wafers/day), such chamber wall conditioning is far more extensive and assured. Thus, we predict that mass spectrometry-based thickness metrology will achieve higher precision in manufacturing application than demonstrated here in a research environment.

Third, because the mass spectrometry-based thickness metrology is obtained in real time, it can be used to drive not only R2R (wafer-to-wafer) control but also real-time end-point process control. While R2R control is proving of profound value in semiconductor manufacturing, it can only compensate for long-term systematic drifts on a wafer-to-wafer basis, while real-time control can compensate for short-term, random variability as well; of course, both are important in manufacturing. We have already demonstrated real-time end-point control of film thickness in a 0.1 Torr SiH_4/WF_6 process for W CVD.[10] The same methodology can be applied in the H_2/WF_6 process at 10 Torr described here, where even better metrological precision has been achieved.

Finally, the specific employment of mass spectrometry sensing to drive metrology and control is synergistic with its well-established use for fault detection in manufacturing. Indeed, mass spectrometry has been implemented on literally hundreds of tools in semiconductor fabs for fault detection and classification, where quantitation is much less demanding but return on investment is high.[1] Here, we have shown that the same sensor that may already be on the tool can be used for high-precision metrology, promising "dual-use sensing" in which the same sensor can drive course correction as well as fault management in the context of APC.

VI. CONCLUSIONS

In situ mass spectrometry sensing has been implemented downstream in a 10 Torr H_2/WF_6 W CVD process to de-

velop a real-time thickness metrology. HF byproduct generation and H_2/WF_6 reactant depletion have been observed in real-time mass spectrometry signals and used to derive predictors of film thickness in synchronism with relevant equipment state signals. Nearly 40 single-wafer runs have been performed to investigate the precision of the mass spectrometry-based thickness metrology under different sets of conditions: (1) a fixed process condition, (2) intentionally introduced R2R process temperature drift, and (3) R2R deposition time variation. Based on real-time integration of the HF byproduct signal from the sensor and its comparison to post-process *ex situ* measurement of the film weight and thickness, we have demonstrated that the precision of this real-time film thickness metrology delivers better than 1% average uncertainty in all cases.

This represents a significant improvement over our previous metrology results in sub-Torr W CVD processes (i.e., 7% average uncertainty in H_2/WF_6 process[11] and 2% average uncertainty in SiH_4/WF_6 process[10]). The improved accuracy is attributed to the increased reactant conversion rate of around 30%, compared to 3% in H_2/WF_6 process[11] and 20% in SiH_4/WF_6 process.[10] The metrological precision—better than 1% average uncertainty—is consistent with industry and roadmap requirements[7] for manufacturing application of advanced process control, particularly in the form of real-time end-point control. Furthermore, we anticipate that the high throughput of manufacturing tools will improve chamber wall conditioning reproducibility compared to our experiments, leading to further improvement of the metrological precision.

The availability of an information-rich, *in situ* chemical sensor—mass spectrometry—capable of real-time, high precision process and wafer state metrology, expands sensor applications for course correction to include real-time as well as R2R control, with benefit in compensation for short-term variability as well as long-term systematic drift in process and equipment. Because mass spectrometry is already a widely deployed sensor for fault detection and classification,[1] it promises dual-use in both components of APC: course correction and fault management.

ACKNOWLEDGMENTS

The authors thank Dr. Robert Ellefson, Dr. Louis Frees and others at Inficon, Inc. for the generous donation of the mass spectrometry sensor equipment, technical interactions, and support of this research. This work has also been supported through the Chemical Science and Technology Laboratory at the National Institute for Standards and Technology.

[1] G. W. Rubloff, *Characterization and Metrology for ULSI Technology: 2003 International Conference*, Austin, TX, 2003 (AIP, Melville, 2003).
[2] S. Cho, *AEC/APC Symposium XV*, Colorado Springs, CO, 2003 (Sematech, Austin, 2003).
[3] T. Sonderman, M. Miller, and C. Bode, Future Fab International **12**, 119 (2002).
[4] S. W. Butler, *Characterization and Metrology for ULSI Technology: 1998 International Conference*, Gaithersburg, MD, 1998 (AIP, Melville, 1998), p. 47.
[5] S. W. Butler, J. Hosch, A. C. Diebold, and B. V. Eck, Future Fab International **1**, 315 (1997).
[6] S. W. Butler, J. Vac. Sci. Technol. B **13**, 1917 (1995).
[7] *International Technology Roadmap for Semiconductors: 2002 Update* (International Sematech, Austin, TX, 2002).
[8] A. C. Diebold, in *Handbook of Silicon Semiconductor Metrology*, edited by A. C. Diebold (Marcel Dekker, New York, 2001), Chap. 7, pp. 143–148.
[9] Integrated Measurement Association, http://www.integratedmeasurement.com
[10] Y. Xu, T. Gougousi, L. Henn-Lecordier, Y. Liu, S. Cho, and G. W. Rubloff, J. Vac. Sci. Technol. B **20**, 2351 (2002).
[11] T. Gougousi, Y. Xu, J. N. Kidder, G. W. Rubloff, and C. R. Tilford, J. Vac. Sci. Technol. B **18**, 1352 (2000).
[12] R. Sreenivasan, T. Gougousi, Y. Xu, J. N. Kidder, E. Zafiriou, and G. W. Rubloff, J. Vac. Sci. Technol. B **19**, 1931 (2001).
[13] T. Gougousi, R. Sreenivasan, Y. Xu, L. Henn-Lecordier, G. W. Rubloff, J. N. Kidder, and E. Zafiriou, *Characterization and Metrology for ULSI Technology: 2000 International Conference*, Gaithersburg, MD, 2000 (AIP, Melville, 2001), p. 249.
[14] G. Lu, L. L. Tedder, and G. W. Rubloff, J. Vac. Sci. Technol. B **17**, 1417 (1999).
[15] L. L. Tedder, G. W. Rubloff, B. F. Cohaghan, and G. N. Parsons, J. Vac. Sci. Technol. A **14**, 267 (1996).
[16] L. L. Tedder, G. W. Rubloff, I. Shareef, M. Anderle, D.-H. Kim, and G. N. Parsons, J. Vac. Sci. Technol. B **13**, 1924 (1995).
[17] X. Li, M. Schaepkens, G. S. Oehrlein, R. E. Ellefson, L. C. Frees, N. Mueller, and N. Komer, J. Vac. Sci. Technol. A **17**, 2438 (1999).
[18] R. W. Cheek, J. A. Kelber, J. G. Fleming, R. S. Blewer, and R. D. Lujan, J. Electrochem. Soc. **140**, 3588 (1993).
[19] L. Henn-Lecordier, J. N. Kidder, G. W. Rubloff, C. A. Gogol, and A. Wajid, J. Vac. Sci. Technol. A **19**, 621 (2001).
[20] S. Yamamoto, K. Nagata, S. Sugai, A. Sengoku, Y. Matsukawa, T. Hattori, and S. Oda, Jpn. J. Appl. Phys., Part 1 **38**, 4727 (1999).
[21] J. Pei, F. L. Degertekin, B. T. Khuri-Yakub, and K. C. Saraswat, Appl. Phys. Lett. **66**, 2177 (1995).
[22] M. G. Flynn, R. Smith, P. Abraham, and S. DenBaars, IEEE Trans. Control Syst. Technol. **9**, 728 (2001).
[23] B. J. Rappoli and W. J. DeSisto, Appl. Phys. Lett. **68**, 2726 (1996).
[24] J. A. O'Neill, M. L. Passow, and T. J. Cotler, J. Vac. Sci. Technol. A **12**, 839 (1994).
[25] K. Hanaoka, H. Ohnishi, and K. Tachibana, Jpn. J. Appl. Phys., Part 1 **32**, 4774 (1993).
[26] J. J. Hsieh and R. V. Joshi, in *Advanced Metallization for ULSI Applications* (Materials Research Society, Pittsburg, PA, 1992), pp. 77–83.
[27] J. J. Hsieh, J. Vac. Sci. Technol. A **11**, 3040 (1993).
[28] H.-Y. Chang, R. A. Adomaitis, J. N. Kidder, and G. W. Rubloff, J. Vac. Sci. Technol. B **19**, 230 (2001).
[29] L. Henn-Lecordier, J. N. Kidder, G. W. Rubloff, C. A. Gogol, and A. Wajid, J. Vac. Sci. Technol. B **21**, 1055 (2003).